



Dioxygenase catalysis by d^0 metal–catecholate complexes containing vanadium and molybdenum with $H_2(3,5\text{-DTBC})$ and $H_2(3,6\text{-DTBC})$ substrates

Aimee M. Morris^a, Cortlandt G. Pierpont^{b,*}, Richard G. Finke^{a,**}

^a Department of Chemistry, Colorado State University, Fort Collins, CO 80523-1872, United States

^b Department of Chemistry and Biochemistry, University of Colorado, Boulder, CO 80309, United States

ARTICLE INFO

Article history:

Received 16 April 2009

Received in revised form 8 May 2009

Accepted 11 May 2009

Available online 20 May 2009

Keywords:

Dioxygenase catalysis

Vanadium precatalyst

Molybdenum precatalyst

Catechol oxidation

ABSTRACT

Facile synthetic dioxygenases, catalysts that can split O_2 and place both oxygen atoms selectively into 2 olefins to yield 2 epoxides or into 2 C–H bonds to yield 2 alcohols, remain a “Holy Grail” of oxidation catalysis. Recently, it was shown that $[VO(3,5\text{-DTBC})(3,5\text{-DBSQ})_2]$ (where 3,5-DTBC and 3,5-DBSQ are 3,5-di-*tert*-butylcatecholate and 3,5-di-*tert*-butylsemiquinone, respectively) is the catalytic-cycle resting state of a record catalytic lifetime catechol dioxygenase catalyst (100,000 total catalytic turnovers) for the substrate 3,5-di-*tert*-butylcatechol, $H_2(3,5\text{-DTBC})$ [C.-X. Yin, R.G. Finke, J. Am. Chem. Soc. 127 (2005) 9003–9013]. Herein we show that the precatalyst $V(3,6\text{-DTBC})_2(3,6\text{-DBSQ})$ also gives dioxygenase products for the substrate $H_2(3,5\text{-DTBC})$, notably the same dioxygenase products in similar yields as seen for $[VO(3,5\text{-DTBC})(3,5\text{-DBSQ})_2]$. EPR studies show that the same $g = 2.003\text{--}2.004$ species are present in solution throughout the oxidation reaction for both $[VO(3,5\text{-DTBC})(3,5\text{-DBSQ})_2]$ and $V(3,6\text{-DTBC})_2(3,6\text{-DBSQ})$. The similar products, product yields, and EPR spectra observed suggest that both $[VO(3,5\text{-DTBC})(3,5\text{-DBSQ})_2]$ and $V(3,6\text{-DTBC})_2(3,6\text{-DBSQ})$ are feeding into the same catalytic cycle. In addition we have expanded the substrates to include $H_2(3,6\text{-DTBC})$, a substrate of interest for its higher symmetry, structurally simplified organic products and steric hindrance expected to favor the formation of monomeric metal–catecholate complexes. The precatalysts $[VO(3,5\text{-DTBC})(3,5\text{-DBSQ})_2]$ and $V(3,6\text{-DTBC})_2(3,6\text{-DBSQ})$ were examined with $H_2(3,6\text{-DTBC})$ and found to give the same intradiol and extradiol dioxygenase products in the same yields. EPR studies of $[VO(3,5\text{-DTBC})(3,5\text{-DBSQ})_2]$ and $V(3,6\text{-DTBC})_2(3,6\text{-DBSQ})$ with $H_2(3,6\text{-DTBC})$ show that the same spectra are observed throughout the oxidation, but at different reaction times. These EPR observations, along with the product studies, suggest that $[VO(3,5\text{-DTBC})(3,5\text{-DBSQ})_2]$ and $V(3,6\text{-DTBC})_2(3,6\text{-DBSQ})$ have a common mechanistic cycle en route to the $H_2(3,6\text{-DTBC})$ dioxygenase products, albeit a mechanism different than that observed for $H_2(3,5\text{-DTBC})$ based on observed EPR spectra and differing product distributions. We also show that oxidation catalysis with $[MoO(3,5\text{-DTBC})_2]$ follows primarily an oxidase path leading to the undesired benzoquinone autooxidation products for both $H_2(3,5\text{-DTBC})$ and $H_2(3,6\text{-DTBC})$ and with reaction times one to two orders of magnitude longer than seen for the vanadium precatalysts. The dramatic difference in product distribution and slower rate for $[MoO(3,5\text{-DTBC})_2]$, along with its lack of a semiquinone ligand in at least this precatalyst, suggests the hypothesis that the d^0 vanadium(V) bonded to a semiquinone ligand in $[VO(3,5\text{-DTBC})(3,5\text{-DBSQ})_2]$ and $V(3,6\text{-DTBC})_2(3,6\text{-DBSQ})$ is a necessary component of these dioxygenase precatalysts able to produce primarily dioxygenase products.

© 2009 Elsevier B.V. All rights reserved.

1. Introduction

Dioxygenases are an important class of catalysts able, by definition, to insert both atoms of O_2 into a substrate without the use of protons and electrons and hence, without the production of side

products. Dioxygenase enzymes exist in nature but selective and facile synthetic dioxygenases that can do difficult reactions such as those shown in Scheme 1 remain a grand challenge or so-called “Holy Grail” in oxidation catalysis [1].

Catechol dioxygenases are a subset of dioxygenases that catalyze the degradation of aromatic compounds via intradiol or extradiol cleavage, Scheme 2. Synthetic catechol dioxygenases have been developed containing Fe(II/III) [2], V(IV/V) [3–7], Ru(II) [8], Rh(III) [9], and other metals [10].

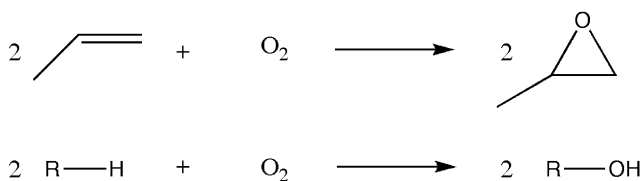
In 1999 a V-containing precatalyst was reported to exhibit a record catalytic lifetime of more than 100,000 total turnovers

* Corresponding author. Tel.: +1 303 492 8420; fax: +1 303 492 0951.

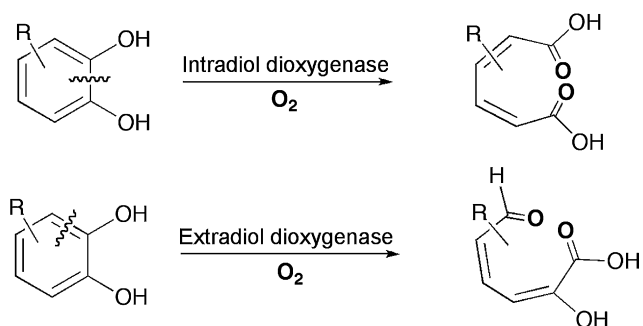
** Corresponding author. Tel.: +1 970 491 2541; fax: +1 970 491 1801.

E-mail addresses: pierpont@colorado.edu (C.G. Pierpont),

rfinke@lamar.colostate.edu (R.G. Finke).



Scheme 1. Desired "Holy Grail" dioxygenase reactions.



Scheme 2. Intradiol vs. extradiol cleavage by catechol dioxygenases.

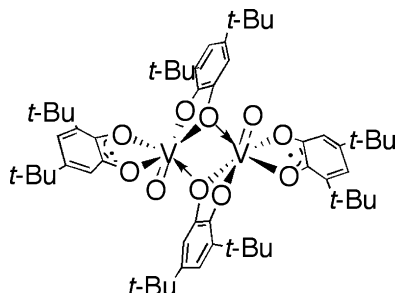


Fig. 1. The catalytic-cycle resting state $[\text{VO}(3,5\text{-DTBC})(3,5\text{-DBSQ})]_2$.

with the substrate 3,5-di-*tert*-butylcatechol, $\text{H}_2(3,5\text{-DTBC})$ [4].¹ It was subsequently determined that 11 different V-containing catechol dioxygenase precatalysts all give a common component or catalytic-cycle resting state of $[\text{VO}(3,5\text{-DTBC})(3,5\text{-DBSQ})]_2$, where 3,5-DTBC = 3,5-di-*tert*-butylcatecholate (which is the deprotonated form of the catechol $\text{H}_2(3,5\text{-DTBC})$) and 3,5-DBSQ = 3,5-di-*tert*-butylsemiquinone, Fig. 1 [5]. The 11 different V-containing precatalysts were shown to form $[\text{VO}(3,5\text{-DTBC})(3,5\text{-DBSQ})]_2$ under the dioxygenase conditions [5,6] to produce both intradiol and extradiol oxidation products from $\text{H}_2(3,5\text{-DTBC})$ [6,7]. These observations have led to interest in whether other related d^0 metal–catecholate complexes might also be able to produce $\text{H}_2(3,5\text{-DTBC})$ dioxygenase products, what the minimum requirements might be for such catechol dioxygenases, and whether the presence of a semiquinone ligand such as 3,5-DBSQ might be important.

We recently reported the synthesis and characterization of a related metal–catecholate complex, $\text{V}(3,6\text{-DTBC})_2(3,6\text{-DBSQ})$ [11]. The complex $\text{V}(3,6\text{-DTBC})_2(3,6\text{-DBSQ})$ is similar to $[\text{VO}(3,5\text{-DTBC})(3,5\text{-DBSQ})]_2$ in that it contains catecholate and semiquinone (SQ) ligands in addition to d^0 V(V). As noted in structural studies of complexes containing 3,6-DTBC and 3,6-DBSQ, the presence

¹ Abbreviations: $\text{H}_2(3,5\text{-DTBC})$ = 3,5-di-*tert*-butylcatechol; 3,5-DTBC = 3,5-di-*tert*-butylcatecholate, the deprotonated form of $\text{H}_2(3,5\text{-DTBC})$; 3,5-DBSQ = 3,5-di-*tert*-butylsemiquinone; $\text{H}_2(3,6\text{-DTBC})$ = 3,6-di-*tert*-butylcatechol; 3,6-DTBC = 3,6-di-*tert*-butylcatecholate; 3,6-DBSQ = 3,6-di-*tert*-butylsemiquinone; SQ = semiquinone; spiro product = spiro[1,4-benzodioxin-2(3H),2'-(2H)-pyran]-3-one,4',6',8-tetrakis(1,1-dimethylethyl); rds = rate determining step.

of *tert*-butyl substituents at ring positions adjacent to donor oxygen atoms blocks bridging to adjacent metals of the type found for $[\text{VO}(3,5\text{-DTBC})(3,5\text{-DBSQ})]_2$ [12]. Such blocking should, in turn, permit studies on the potential importance of the dimeric structure of $[\text{VO}(3,5\text{-DTBC})(3,5\text{-DBSQ})]_2$ on dioxygenase activity. The symmetrical $\text{H}_2(3,6\text{-DTBC})$ should also lead to a less complicated series of organic oxidation products relative to $\text{H}_2(3,5\text{-DTBC})$, but possibly at the expense of the catalytic activity. In fact, in an earlier study using an iron catalyst, Funabiki and co-workers found that an Fe complex containing 3,6-DTBC had significantly lower oxidation activity than did the same Fe complex with a 3,5-DTBC ligand [11].

An additional d^0 metal–catecholate complex, $[\text{MoO}(3,5\text{-DTBC})_2]_2$, was reported in 1979 as the product of O_2 addition to $\text{Mo}(3,5\text{-DTBC})_3$ [13]. $[\text{MoO}(3,5\text{-DTBC})_2]_2$ is of interest since it has a dimeric structure that is identical to $[\text{VO}(3,5\text{-DTBC})(3,5\text{-DBSQ})]_2$. The metal ion (Mo(VI)) is also d^0 , but the ligands are now all catecholates, a feature which permits a test of the importance of a semiquinone ligand in at least the precatalyst en route to obtaining dioxygenase products.

Herein we report the catechol dioxygenase activity for the d^0 precatalysts $[\text{VO}(3,5\text{-DTBC})(3,5\text{-DBSQ})]_2$, $\text{V}(3,6\text{-DTBC})_2(3,6\text{-DBSQ})$, and $[\text{MoO}(3,5\text{-DTBC})_2]_2$ with both $\text{H}_2(3,5\text{-DTBC})$ and $\text{H}_2(3,6\text{-DTBC})$ as substrates. In addition to examining whether $\text{V}(3,6\text{-DTBC})_2(3,6\text{-DBSQ})$ and $[\text{MoO}(3,5\text{-DTBC})_2]_2$ are able to produce dioxygenase products for both the $\text{H}_2(3,5\text{-DTBC})$ and $\text{H}_2(3,6\text{-DTBC})$ substrates, it is of interest to determine if these precatalysts lead to the dioxygenase mechanism proposed [6,7] for $[\text{VO}(3,5\text{-DTBC})(3,5\text{-DBSQ})]_2$ in which half of this dimeric complex is involved in the actual catalytic cycle.

2. Results and discussion

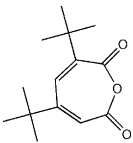
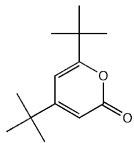
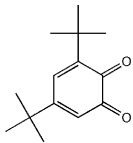
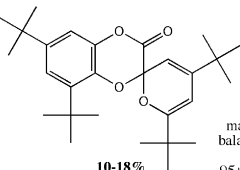
2.1. O_2 -uptake by solutions of $\text{H}_2(3,5\text{-DTBC})$ with precatalysts $[\text{VO}(3,5\text{-DTBC})(3,5\text{-DBSQ})]_2$, $\text{V}(3,6\text{-DTBC})_2(3,6\text{-DBSQ})$, or $[\text{MoO}(3,5\text{-DTBC})_2]_2$

Dioxygen uptake plots for solutions containing $\text{H}_2(3,5\text{-DTBC})$ and the precatalysts $[\text{VO}(3,5\text{-DTBC})(3,5\text{-DBSQ})]_2$, $\text{V}(3,6\text{-DTBC})_2(3,6\text{-DBSQ})$, and $[\text{MoO}(3,5\text{-DTBC})_2]_2$ are shown in Fig. 2. Experiments were carried out with 1.8 mmol of $\text{H}_2(3,5\text{-DTBC})$, 1–2 μmol of precatalyst, 8.2 mL of 1,2-dichloroethane, 40 °C, and 0.8 atm of O_2 . Fig. 2a shows representative O_2 -uptake curves for the precatalysts $[\text{VO}(3,5\text{-DTBC})(3,5\text{-DBSQ})]_2$ and $\text{V}(3,6\text{-DTBC})_2(3,6\text{-DBSQ})$ and reveals that these two V-precatalysts behave identical kinetically. In Fig. 2b, comparison of the O_2 -uptake time by the two V-precatalysts to that of $[\text{MoO}(3,5\text{-DTBC})_2]_2$ reveals that the $[\text{VO}(3,5\text{-DTBC})(3,5\text{-DBSQ})]_2$ or $\text{V}(3,6\text{-DTBC})_2(3,6\text{-DBSQ})$ precatalysts are roughly two orders of magnitude faster than the $[\text{MoO}(3,5\text{-DTBC})_2]_2$ precatalyst.

2.2. Observed $\text{H}_2(3,5\text{-DTBC})$ dioxygenase plus oxidase products and their yields from the O_2 -uptake reactions

At the end of each O_2 -uptake reaction with $\text{H}_2(3,5\text{-DTBC})$, the reaction solution was analyzed by gas chromatography (GC) in comparison to authentic samples as described in Section 4. Scheme 3 shows the respective $\text{H}_2(3,5\text{-DTBC})$ intradiol and extradiol dioxygenase products plus any benzoquinone oxidase product, along with their yields, observed for the precatalysts $[\text{VO}(3,5\text{-DTBC})(3,5\text{-DBSQ})]_2$, $\text{V}(3,6\text{-DTBC})_2(3,6\text{-DBSQ})$, and $[\text{MoO}(3,5\text{-DTBC})_2]_2$.

The data show that $[\text{VO}(3,5\text{-DTBC})(3,5\text{-DBSQ})]_2$ and $\text{V}(3,6\text{-DTBC})_2(3,6\text{-DBSQ})$ give the same dioxygenase products in similar yields for the first two products in Scheme 3, but that $\text{V}(3,6\text{-DTBC})_2(3,6\text{-DBSQ})$ with its sterically more crowded 3,6-DTBC ligand gives more of the benzoquinone autoxidation product and

					mass balance	reaction time
[VO(3,5-DTBC)(3,5-DBSQ)] ₂	40–57%	6–15%	9–25%	10–18%	95±5%	5±2 hrs
V(3,6-DTBC) ₂ (3,6-DBSQ)	45–55%	10–11%	29–43%	2–4%	95±5%	3.5±1.5 hrs
[MoO(3,5-DTBC) ₂] ₂	16%	1%	56%	3%	76% ^a	~330 hrs

^a The 76% (i.e., <100%) mass balance is likely a result of product follow-up reactions and/or decomposition during the required long reaction times.

Scheme 3. H₂(3,5-DTBC) dioxygenase products and yields observed for the precatalysts [VO(3,5-DTBC)(3,5-DBSQ)]₂, V(3,6-DTBC)₂(3,6-DBSQ), or [MoO(3,5-DTBC)₂]₂ in comparison to calibration by authentic samples. A range of observed yields (minimum and maximum observed yields) from repeat experiments is given. In the case of the precatalyst [VO(3,5-DTBC)(3,5-DBSQ)]₂, the range of yields given includes those observed from prior as well as the present work [7] (i.e., and therefore includes the full range of yields anyone repeating this work is likely to encounter, and so long as identical conditions are employed).

less of the (somewhat sterically crowded) spiro product, spiro[1,4-benzodioxin-2(3*H*),2'-(2*H*)-pyran]-3-one,4',6,6',8-tetrakis(1,1-dimethylethyl). On the other hand, the molybdenum complex [MoO(3,5-DTBC)₂]₂ exhibits quite different reactivity: in addition to taking two orders of magnitude longer to complete the

O₂-uptake (Fig. 2b), it gives a majority (56%) of the autoxidation product, benzoquinone, Scheme 3.

The results displayed in Scheme 3 show that V(3,6-DTBC)₂(3,6-DBSQ) is also an effective dioxygenase precatalyst for the H₂(3,5-DTBC) substrate, albeit one that gives higher yields of the undesired benzoquinone autoxidation product and lower yields of the spiro complex. More interesting is that the slow O₂-uptake and primarily non-dioxygenase products seen for [MoO(3,5-DTBC)₂]₂ suggest, in comparison to the results for the V-based precatalysts, that either (i) the presence of the SQ ligand in both [VO(3,5-DTBC)(3,5-DBSQ)]₂ and V(3,6-DTBC)₂(3,6-DBSQ) is an important and necessary component of these precatalysts for their faster catalysis to the observed H₂(3,5-DTBC) dioxygenase products, or that (ii) the first row V rather than second row Mo as the d⁰ metal is important for the observed catalysis since reaction rates of *catechol oxidations* for second row metals are often orders of magnitude slower than for first row metals [14]. Regardless of the precise details and explanation here, the observed results demonstrate that the presence of a d⁰ vanadium bonded to a semiquinone ligand is a preferred precatalyst combination (vs. d⁰ Mo bonded to catecholates) for the formation of high yields of the H₂(3,5-DTBC) dioxygenase products.

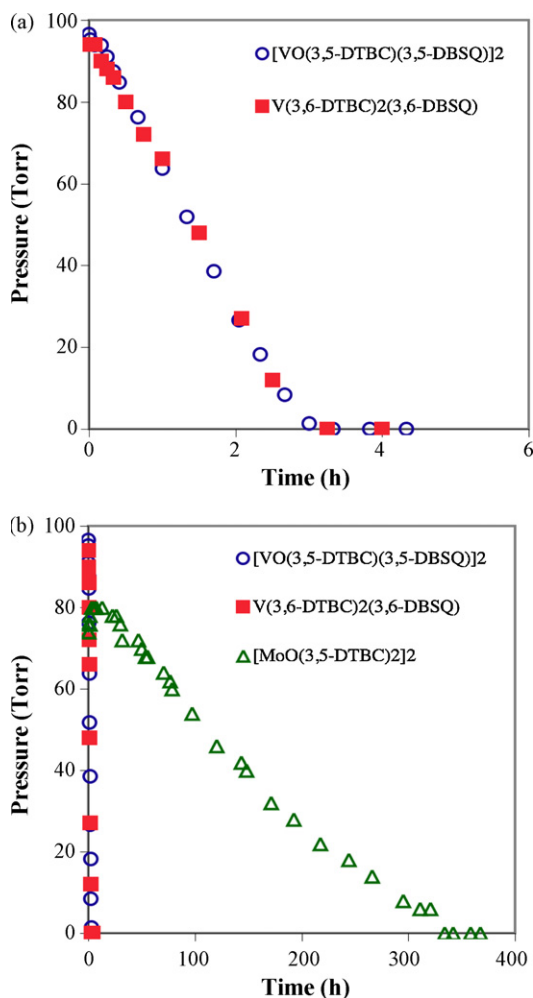


Fig. 2. (a) The time region between 0 and 6 h for the precatalysts [VO(3,5-DTBC)(3,5-DBSQ)]₂ and V(3,6-DTBC)₂(3,6-DBSQ) plus H₂(3,5-DTBC). (b) Three separate representative O₂-uptake curves of the substrate H₂(3,5-DTBC) plus the precatalyst [VO(3,5-DTBC)(3,5-DBSQ)]₂, V(3,6-DTBC)₂(3,6-DBSQ), and [MoO(3,5-DTBC)₂]₂ on a ca. 6.6-fold expanded time scale vs. (a). The greatly, ca. 102-fold faster rate of the [VO(3,5-DTBC)(3,5-DBSQ)]₂ and V(3,6-DTBC)₂(3,6-DBSQ) systems is apparent. The conditions are as follows: 1.8 mmol of substrate, 1–2 μmol of precatalyst, 8.2 mL of 1,2-dichloroethane, 40 °C, and 0.8 atm of O₂. Note that the final pressure in each case has been subtracted from each data point, so that the net pressure loss to a zero final pressure is shown here and in analogous figures hereafter.

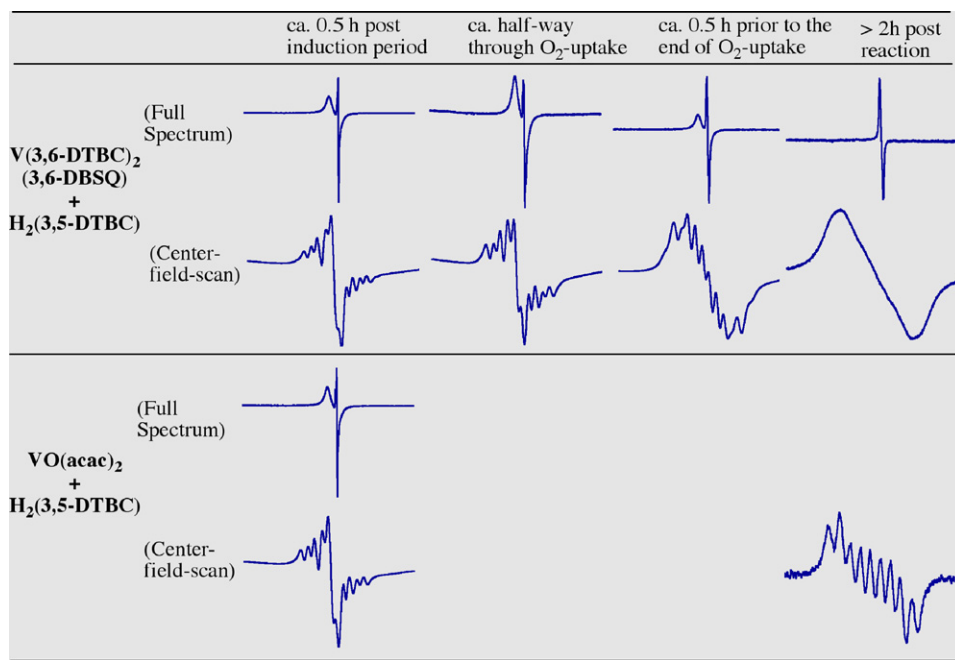
2.3. Time-dependent EPR studies of H₂(3,5-DTBC) plus V(3,6-DTBC)₂(3,6-DBSQ)

Electron paramagnetic resonance (EPR) spectroscopy was used to follow the paramagnetic species present in solution during the O₂-uptake of H₂(3,5-DTBC) with the V(3,6-DTBC)₂(3,6-DBSQ) precatalyst. Table 1 displays changes in the observed EPR spectra throughout the O₂-uptake. Initially, a scan of the full 1000 G spectrum shows a broad signal at $g = 2.030\text{--}2.031$ along with a signal at $g = 2.003\text{--}2.004$ at its center-field, Table 1. A center-field scan at 50 G reveals a 10-line spectrum ($g = 2.006$, $A(^{51}\text{V}) = 2.1$ G) that matches the 10-line spectrum previously observed for the [VO(3,5-DTBC)(3,5-DBSQ)]₂ precursor VO(acac)₂ plus H₂(3,5-DTBC) [5]. The 10-line spectrum was previously assigned to “V(3,5-DBSQ)₃” formed by the addition of H₂(3,5-DTBC) to either V(CO)₆ or VO(acac)₂ [13]. However, “V(3,5-DBSQ)₃” with a parent ion peak at $m/z = 712$ [13] may have actually been V(3,5-DTBC)₂(3,5-DBSQ) based on the recently solved structure of V(3,6-DTBC)₂(3,6-DBSQ) [11]. As the O₂-uptake progresses, the broad signal at $g = 2.030\text{--}2.031$ becomes more intense and then disappears by the end of the reaction suggesting that this broad signal is associated with an active dioxygenase catalyst—that is, this signal does behave as expected for a kinetically competent intermediate. The line-width of the broad signal suggests that the species is a V(V)-bound radical with unresolved hyperfine coupling.

Furthermore, the center-field signal changes from a 10-line spectrum to a 9-line spectrum. This 9-line spectrum with $g = 2.004$ and

Table 1

Time-dependent EPR spectra of $V(3,6\text{-DTBC})_2(3,6\text{-DBSQ})$ plus $H_2(3,5\text{-DTBC})$ under oxidation conditions in toluene compared to the EPR spectra previously reported [5] for $VO(acac)_2$ plus $H_2(3,5\text{-DTBC})$ under otherwise identical experimental conditions^a.



^a The full spectra were scanned at a magnetic field width of 1000 G while the center-field scans were over 50 G.

$A(^{51}V) = 3.0\text{ G}$, characteristic of a single semiquinone ligand coupled to a ^{51}V center, is consistent with the EPR spectrum due to $[VO(3,5\text{-DTBC})(3,5\text{-DBSQ})]_2$ that is also observed at the end of the O_2 -uptake reaction of $VO(acac)_2$ plus $H_2(3,5\text{-DTBC})$ [5], Table 1. This suggests that during the O_2 -uptake of $V(3,6\text{-DTBC})_2(3,6\text{-DBSQ})$ plus $H_2(3,5\text{-DTBC})$, the previously proposed [6] catalytic-cycle resting state of $[VO(3,5\text{-DTBC})(3,5\text{-DBSQ})]_2$ is formed. This in turn suggests that the catalytic cycle previously seen, in which $[VO(3,5\text{-DTBC})(3,5\text{-DBSQ})]_2$ breaks in half and then reacts with O_2 in a rate-determining step [6], is also accessed in the $V(3,6\text{-DTBC})_2(3,6\text{-DBSQ})$ plus $H_2(3,5\text{-DTBC})$ reaction, perhaps not unexpectedly due to the presence of a large excess of the $H_2(3,5\text{-DTBC})$ substrate over the $V(3,6\text{-DTBC})_2(3,6\text{-DBSQ})$ precatalyst.

Finally, after the O_2 -uptake reaction is complete, a one-line spectrum of $g = 2.003$ is observed, Table 1. This one-line spectrum may be a result of a monomeric $VO(DTBC)(DBSQ)$ species that has intramolecular electron transfer occurring on the EPR timescale between symmetrically equivalent catechol ligands, thereby causing the loss of hyperfine coupling as has been observed in Co-catecholate complexes [15].

The fact that the same 10-line and 9-line spectra are observed during the O_2 -uptake of $H_2(3,5\text{-DTBC})$ with either the $[VO(3,5\text{-DTBC})(3,5\text{-DBSQ})]_2$ precursor $VO(acac)_2$ or $V(3,6\text{-DTBC})_2(3,6\text{-DBSQ})$, along with the same products being observed in similar yields (Scheme 3), strongly suggests that these two precatalysts lead to the same catalyst(s). The time-dependent EPR spectra observed with the $H_2(3,5\text{-DTBC})$ substrate plus $VO(acac)_2$ or $V(3,6\text{-DTBC})_2(3,6\text{-DBSQ})$ as well as the previous evidence for $[VO(3,5\text{-DTBC})(3,5\text{-DBSQ})]_2$ as the catalyst-cycle resting state [6], are all generally consistent with the previously proposed mechanism [6] and catalytic-cycle resting state of $[VO(3,5\text{-DTBC})(3,5\text{-DBSQ})]_2$. That said, it is unknown at this time precisely how and where the $V(3,6\text{-DTBC})_2(3,6\text{-DBSQ})$ precatalyst feeds into the previously established catalytic cycle, shown in Scheme 4 for $[VO(3,5\text{-DTBC})(3,5\text{-DBSQ})]_2$ plus $H_2(3,5\text{-DTBC})$. Note that based on the product yields given as part of Scheme 3, there is at most a mod-

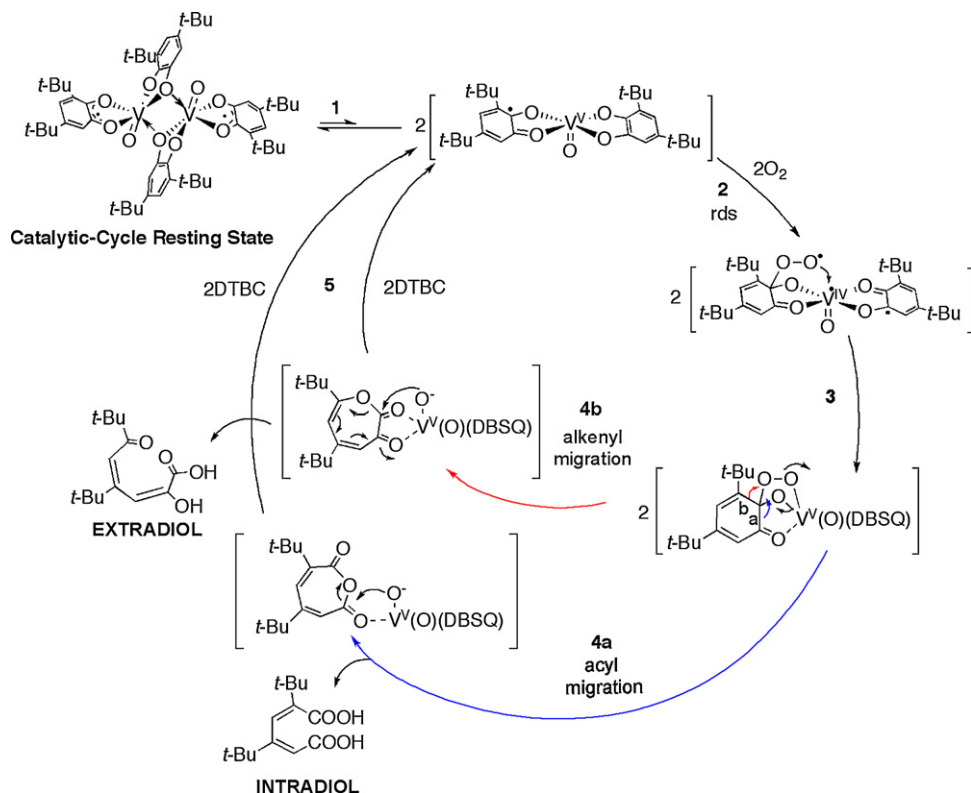
est observed preference ($\leq 1.2\text{--}4.6$ fold) for intradiol over extradiol products, the precise origins of which are not understood [2e].

2.4. O_2 -uptake studies of $H_2(3,6\text{-DTBC})$ with $[VO(3,5\text{-DTBC})(3,5\text{-DBSQ})]_2$, $V(3,6\text{-DTBC})_2(3,6\text{-DBSQ})$, or $[MoO(3,5\text{-DTBC})_2]_2$

We then wondered if the above d^0 metal-catecholate complexes are also dioxygenase catalysts for the more hindered substrate, $H_2(3,6\text{-DTBC})$. Fig. 3 shows the O_2 -uptake curves obtained for the precatalyst $[VO(3,5\text{-DTBC})(3,5\text{-DBSQ})]_2$, $V(3,6\text{-DTBC})_2(3,6\text{-DBSQ})$, or $[MoO(3,5\text{-DTBC})_2]_2$ with the $H_2(3,6\text{-DTBC})$ substrate.

Fig. 3a illustrates that the precatalysts $[VO(3,5\text{-DTBC})(3,5\text{-DBSQ})]_2$ and $V(3,6\text{-DTBC})_2(3,6\text{-DBSQ})$ show similar (slightly sigmoidal) O_2 -uptake curves with similar net reaction times for the oxidation of $H_2(3,6\text{-DTBC})$. Interesting here is the fact that the oxidation rates for the $H_2(3,5\text{-DTBC})$ and $H_2(3,6\text{-DTBC})$ substrates are similar, results which contrast what has been previously observed for an Fe dioxygenase model system containing either a 3,5-DTBC or 3,6-DTBC ligand. The Fe 3,5-DTBC system is very active ($k_{\text{oxidation}} = 18\text{ M}^{-1}\text{ s}^{-1}$) while the 3,6-DTBC complex displays a ca. 820-fold lower reactivity ($k_{\text{oxidation}} = 0.022\text{ M}^{-1}\text{ s}^{-1}$) [16]; hence, the high, but roughly equivalent, reactivity $[VO(3,5\text{-DTBC})(3,5\text{-DBSQ})]_2$ and $V(3,6\text{-DTBC})_2(3,6\text{-DBSQ})$ with $H_2(3,6\text{-DTBC})$ is an interesting finding. The simplest interpretation of these results is that fairly rapid evolution (e.g., via ligand exchange or other, necessary reactions) of each precatalyst to the same catalyst is occurring. Fig. 3b shows that $[MoO(3,5\text{-DTBC})_2]_2$ is slower requiring ca. 1/2 an order of magnitude longer than $[VO(3,5\text{-DTBC})(3,5\text{-DBSQ})]_2$ or $V(3,6\text{-DTBC})_2(3,6\text{-DBSQ})$ for the oxidation of $H_2(3,6\text{-DTBC})$.

In addition to the $H_2(3,6\text{-DTBC})$ substrate, we briefly looked at simple catechol, but found that with the precatalyst $[VO(3,5\text{-DTBC})(3,5\text{-DBSQ})]_2$ no O_2 -uptake under standard conditions was observed even after >2 days (Figure S1 of the Supporting Information). This result reaffirms the established point [1e] that the electron donating *tert*-butyl groups are an important component of



Scheme 4. The previously supported catalytic cycle for the formation of $H_2(3,5\text{-DTBC})$ dioxygenase products starting from $[VO(3,5\text{-DTBC})(3,5\text{-DBSQ})]_2$ [6]. The previously published kinetic and other data revealed that the catalytic-cycle resting state dimer breaks in half and then reacts with O_2 in the rate-determining step (rds) as shown [6]. Steps after the rds (step 2) are, therefore, kinetically hidden and, therefore, had to be written by analogy with prior, seminal work of others [1f,19,20] specifically the literature precedent for steps 3 and 4 [18].

the substrate for facile dioxygenase catalysis to be observed, at least with precatalysts such as $[VO(3,5\text{-DTBC})(3,5\text{-DBSQ})]_2$, a significant limitation of these catalyst systems in terms of the other catechols that one would like to oxygenate via dioxygenase reactions.

2.5. Observed $H_2(3,6\text{-DTBC})$ dioxygenase products and yields from O_2 -uptake reactions with the precatalysts $[VO(3,5\text{-DTBC})(3,5\text{-DBSQ})]_2$, $V(3,6\text{-DTBC})_2(3,6\text{-DBSQ})$, or $[MoO(3,5\text{-DTBC})]_2$

Similar to the dioxygenase products that were previously observed with $H_2(3,5\text{-DTBC})$, both intradiol and extradiol products are also observed at the end of the O_2 -uptake reaction with $H_2(3,6\text{-DTBC})$, although the products are simpler as anticipated. The $H_2(3,6\text{-DTBC})$ dioxygenase products observed and quantified by GC at the end of the O_2 -uptake reactions, in comparison to authentic standards, are shown in Scheme 5. These products were also separated from one another by column chromatography and characterized by 1H and ^{13}C NMR, GC-MS, and X-ray diffraction (See Section 4 as well as the Supporting Information). Those characterized, authentic products were then used to calibrate the GC en route to the reported yields.

Scheme 5 shows that the same products within experimental error are observed for both the $[VO(3,5\text{-DTBC})(3,5\text{-DBSQ})]_2$ and $V(3,6\text{-DTBC})_2(3,6\text{-DBSQ})$ precatalysts. Interestingly, the $H_2(3,6\text{-DTBC})$ substrate shows that a majority (>69%) of the extradiol product is obtained (Scheme 5) as opposed to a majority (>40%) of the intradiol product observed when $H_2(3,5\text{-DTBC})$ is the substrate, Scheme 3, *vide supra*. Furthermore, less of the benzoquinone autoxidation product is observed with the $H_2(3,6\text{-DTBC})$ substrate (1–2%) as opposed to the $H_2(3,5\text{-DTBC})$ substrate (>9%), Schemes 3 and 5. Another difference between the $H_2(3,5\text{-DTBC})$ and $H_2(3,6\text{-DTBC})$

substrates is that no spiro product is observed with $H_2(3,6\text{-DTBC})$, as expected if steric hindrance from the para *t*-butyl groups is inhibiting the formation of an analogous spiro product.

The results in Scheme 5 extend the substrate list for which $[VO(3,5\text{-DTBC})(3,5\text{-DBSQ})]_2$ and $V(3,6\text{-DTBC})_2(3,6\text{-DBSQ})$ act as dioxygenase precatalysts. The results in Scheme 5 also demonstrate that $V(3,6\text{-DTBC})_2(3,6\text{-DBSQ})$ is an equally good dioxygenase for $H_2(3,6\text{-DTBC})$ that produces the same dioxygenase products in the same yields as does $[VO(3,5\text{-DTBC})(3,5\text{-DBSQ})]$. Scheme 5 further demonstrates that with $[MoO(3,5\text{-DTBC})]_2$, and similar to the results for $H_2(3,5\text{-DTBC})$, the $H_2(3,6\text{-DTBC})$ substrate gives primarily (ca. 51% of) the undesired benzoquinone autoxidation product. Furthermore the $[MoO(3,5\text{-DTBC})]_2$ precatalyst is slow enough and eventually deactivates so that 12% of the starting $H_2(3,6\text{-DTBC})$ substrate still remains even ≥ 2 h after no further O_2 -uptake is observed. Even to reach that point, the O_2 -uptake takes half an order of magnitude longer than either of the vanadium catecholate precatalysts.

The implication of these V- vs. Mo-results is, again, that either (i) a semiquinone ligand is important for the dioxygenase catalysis, or that (ii) d^0 vanadium is superior to d^0 molybdenum; or that (iii) both the d^0 vanadium and a semiquinone ligand are crucial for the observed, faster and more efficacious dioxygenase catalysis.

2.6. Time-dependent EPR studies of $H_2(3,6\text{-DTBC})$ with $[VO(3,5\text{-DTBC})(3,5\text{-DBSQ})]_2$, or $V(3,6\text{-DTBC})_2(3,6\text{-DBSQ})$

EPR spectroscopy was once again used to follow the species present in solution during the O_2 -uptake of $H_2(3,6\text{-DTBC})$ with either the precatalyst $[VO(3,5\text{-DTBC})(3,5\text{-DBSQ})]_2$ (top panel, Table 2) or $V(3,6\text{-DTBC})_2(3,6\text{-DBSQ})$ (bottom panel, Table 2). With the $[VO(3,5\text{-DTBC})(3,5\text{-DBSQ})]_2$ precatalyst, an initial scan

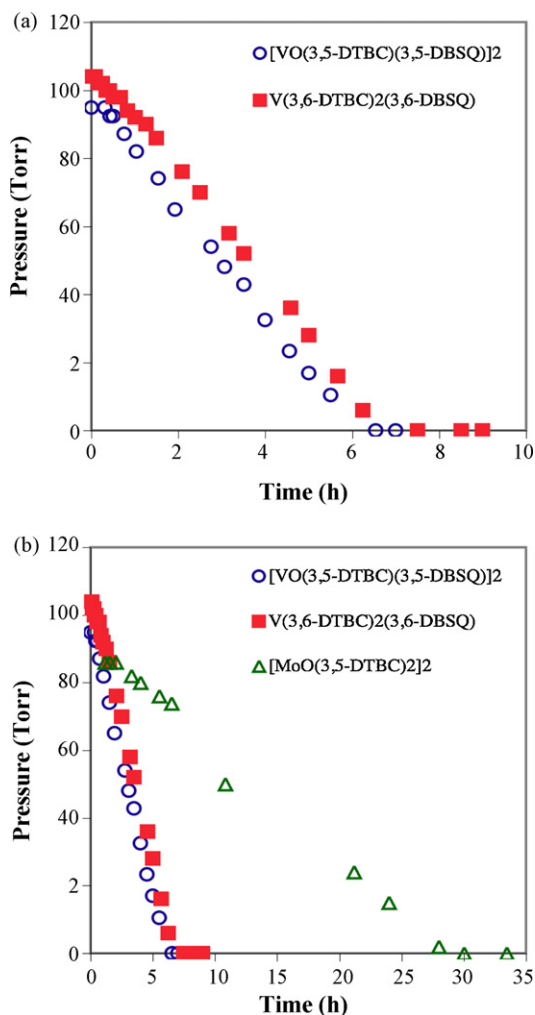


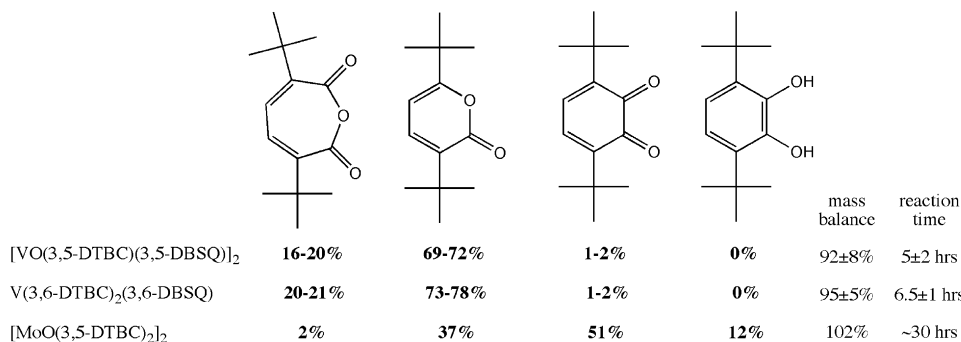
Fig. 3. (a) The precatalyst $[\text{VO}(\text{3,5-DTBC})(\text{3,5-DBSQ})]_2$ or $\text{V}(\text{3,6-DTBC})_2(\text{3,6-DBSQ})$ plus $\text{H}_2(\text{3,6-DTBC})$ O_2 -uptake curves from 0 to 10 h. (b) Representative O_2 -uptake curves of the substrate $\text{H}_2(\text{3,6-DTBC})$ plus the precatalyst $[\text{VO}(\text{3,5-DTBC})(\text{3,5-DBSQ})]_2$, $\text{V}(\text{3,6-DTBC})_2(\text{3,6-DBSQ})$, or $[\text{MoO}(\text{3,5-DTBC})_2]_2$. The conditions are as follows: 1.8 mmol of substrate, 1–2 μmol of precatalyst, 8.2 mL of 1,2-dichloroethane, 40 °C, and 0.8 atm of O_2 . Again, the data reveal that the two V-precatalysts are similar in their kinetics while the Mo-precatalyst is again slower, but now by only ca. 5-fold.

of the full 1000 G spectrum shows a prominent broad signal at $g = 2.026\text{--}2.027$ along with a signal at $g = 2.003\text{--}2.004$ at its center-field, Table 2. A center-field scan at 50 G shows a broad signal with a lack of resolvable hyperfine splitting. As the reaction progresses, the broad signal at $g = 2.026\text{--}2.027$ begins to diminish in

intensity and the center-field signal at $g = 2.003\text{--}2.004$ becomes more apparent. A scan of the center-field shows a six-line spectrum that is likely the result of a triplet split by an additional spin = 1/2 nucleus. The full-spectrum after further O_2 -uptake then displays another more intense signal at $g = 2.026\text{--}2.037$ and the center-field scan begins to lose the hyperfine resolution. After the O_2 -uptake is complete, the broad signal at $g = 2.026\text{--}2.027$ is nearly absent and the prominent signal at $g = 2.003\text{--}2.004$ shows no hyperfine splitting in a center-field scan. Interestingly, the same EPR spectra are observed throughout the O_2 -uptake reaction with the $\text{V}(\text{3,6-DTBC})_2(\text{3,6-DBSQ})$ precatalyst but, again, at different times during the reaction. That is, looking at the full spectrum scans, the broad signal at $g = 2.026\text{--}2.027$ is also observed but it appears to increase in intensity during the reaction and then diminish after the reaction is complete as opposed to the intensity starting off large, decreasing, increasing again, and finally diminishing as seen for $[\text{VO}(\text{3,5-DTBC})(\text{3,5-DBSQ})]_2$. In addition, examination of the center-field scans with $\text{V}(\text{3,6-DTBC})_2(\text{3,6-DBSQ})$ initially shows the same six-line spectrum that is observed near the middle of the O_2 -uptake reaction with $[\text{VO}(\text{3,5-DTBC})(\text{3,5-DBSQ})]_2$. This six-line spectrum then gradually loses the hyperfine coupling throughout the course of the reaction and finally the same simple one-line spectrum with $g = 2.004$ as was observed with $[\text{VO}(\text{3,5-DTBC})(\text{3,5-DBSQ})]_2$, is observed at the end of the O_2 -uptake with $\text{V}(\text{3,6-DTBC})_2(\text{3,6-DBSQ})$.

The fact that the same EPR spectra are observed, but at different reaction times, for $\text{H}_2(\text{3,6-DTBC})$ with both $[\text{VO}(\text{3,5-DTBC})(\text{3,5-DBSQ})]_2$ and $\text{V}(\text{3,6-DTBC})_2(\text{3,6-DBSQ})$ suggests that these two precatalysts are feeding into the same catalytic cycle, at least in the simplest, “Ockham’s razor” interpretation of the data that we observe. We hypothesize that the six-line spectrum that is observed with the $\text{H}_2(\text{3,6-DTBC})$ substrate is a result of the formation of $\text{H}(\text{3,6-DTBC})$ which arises from protonation of one SQ by protons derived from $\text{H}_2(\text{3,6-DTBC})$. The triplet arises from coupling to the two equivalent protons at the 4 and 5 ring positions ($A = 3.9\text{ G}$). Weaker coupling to the proton bound to the oxygen ($A = 1.6\text{ G}$) gives the six lines. The g -value and coupling constants observed for the six-line spectrum match those previously observed for free $\text{H}(\text{3,6-DTBC})$ [17].

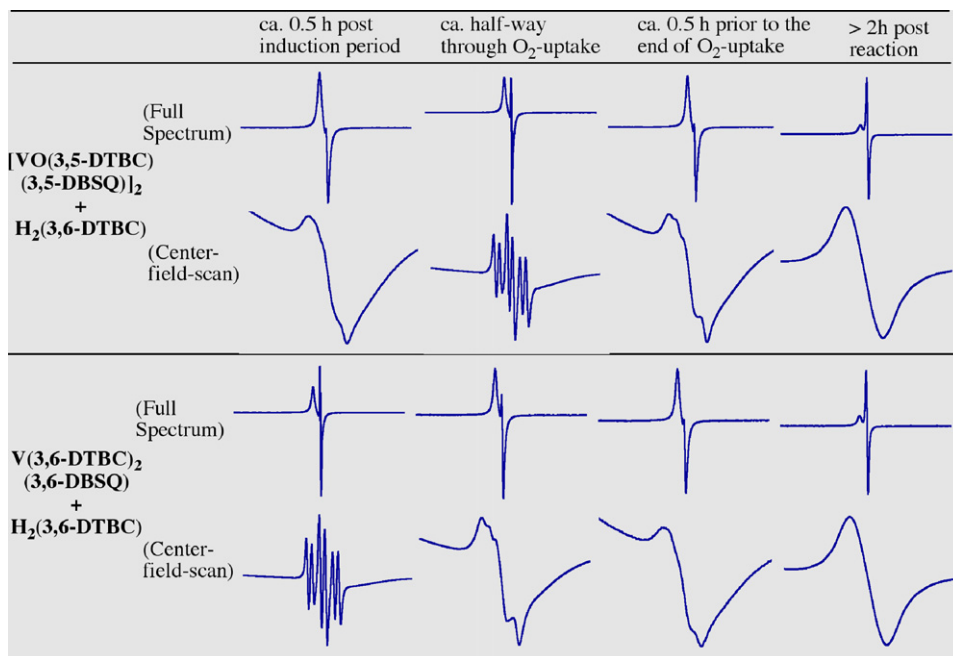
The other center-field spectra that are observed throughout the O_2 -uptake of $\text{H}_2(\text{3,6-DTBC})$ look to be a result of the loss of hyperfine coupling from the six-line spectrum. The asymmetry of the signal suggests overlap of more than one signal. Again as we suggested for the $\text{H}_2(\text{3,5-DTBC})$ substrate, the broad one-line signal observed after the O_2 -uptake is complete for $\text{H}_2(\text{3,6-DTBC})$ plus $[\text{VO}(\text{3,5-DTBC})(\text{3,5-DBSQ})]_2$ or $\text{V}(\text{3,6-DTBC})_2(\text{3,6-DBSQ})$ may be a result of a monomeric $\text{VO}(\text{3,6-DTBC})(\text{3,6-DBSQ})$ species that has intramolecular electron transfer between the symmetrically equivalent 3,6-DTBC and 3,6-DBSQ ligands causing the hyperfine signals to be lost.



Scheme 5. $\text{H}_2(\text{3,6-DTBC})$ dioxxygenase products and product yields. The range of yields shown represents the maximum and minimum yields that were obtained for ≥ 3 separate O_2 -uptake reactions.

Table 2

Time-dependent EPR spectra of the precatalysts $[\text{VO}(\text{3,5-DTBC})(\text{3,5-DBSQ})]_2$ and $\text{V}(\text{3,6-DTBC})_2(\text{3,6-DBSQ})$ with the $\text{H}_2(\text{3,6-DTBC})$ substrate under our stated (See Section 4) standard oxygenation conditions in toluene^a.



^a The full spectra were scanned at a magnetic field width of 1000 G while the center-field scans were obtained at 50 G.

Overall, the EPR spectra shown in Table 2 along with the observed products and yields (Scheme 5) suggest that both the precatalysts $[\text{VO}(\text{3,5-DTBC})(\text{3,5-DBSQ})]_2$ and $\text{V}(\text{3,6-DTBC})_2(\text{3,6-DBSQ})$ are feeding into the same dioxygenase catalytic cycle. It also appears by the difference in EPR spectra, as well as the difference in intradiol vs. extradiol products observed, that the $\text{H}_2(\text{3,6-DTBC})$ substrate may be operating under a different mechanism in comparison to the $\text{H}_2(\text{3,5-DTBC})$ substrate (Scheme 4) for the formation of dioxygenase products. However, further kinetic, spectroscopic and other studies probing the mechanism of $\text{H}_2(\text{3,6-DTBC})$ with $[\text{VO}(\text{3,5-DTBC})(\text{3,5-DBSQ})]_2$ and $\text{V}(\text{3,6-DTBC})_2(\text{3,6-DBSQ})$ precatalysts will be needed to gain deeper insights into the mechanism underlying the $\text{H}_2(\text{3,6-DTBC})$ oxidation pathway(s).

3. Conclusions

The main findings from this study can be summarized as follows:

- Product studies reveal that, as with $[\text{VO}(\text{3,5-DTBC})(\text{3,5-DBSQ})]_2$ before [5–7], $\text{V}(\text{3,6-DTBC})_2(\text{3,6-DBSQ})$ is an effective dioxygenase precatalyst for the substrate $\text{H}_2(\text{3,5-DTBC})$. The precatalyst $\text{V}(\text{3,6-DTBC})_2(\text{3,6-DBSQ})$ generally gives two primary dioxygenase products in similar yields, but also gives a higher yield of the undesired benzoquinone autoxidation product and a lower yield of the spiro complex in comparison to beginning with $[\text{VO}(\text{3,5-DTBC})(\text{3,5-DBSQ})]_2$.
- Time-dependent EPR studies show that similar species are observed in solution throughout the O_2 -uptake using either $[\text{VO}(\text{3,5-DTBC})(\text{3,5-DBSQ})]_2$ or $\text{V}(\text{3,6-DTBC})_2(\text{3,6-DBSQ})$ plus $\text{H}_2(\text{3,5-DTBC})$. Specifically, a 10-line spectrum corresponding to “ $\text{V}(\text{3,5-DBSQ})_3$ ” [13], as well as a 9-line spectrum corresponding to $[\text{VO}(\text{3,5-DTBC})(\text{3,5-DBSQ})]_2$, are both observed regardless of which precatalyst is used. However, the EPR spectra are observed at different times during the reaction, results which require different kinetics en route to the observed species.

- The EPR studies along with the observed similar products and yields suggest that $[\text{VO}(\text{3,5-DTBC})(\text{3,5-DBSQ})]_2$ and $\text{V}(\text{3,6-DTBC})_2(\text{3,6-DBSQ})$ plus $\text{H}_2(\text{3,5-DTBC})$ are operating predominantly by the same, mostly likely previously established [6] mechanism.
- We have also expanded the list of substrates to include $\text{H}_2(\text{3,6-DTBC})$ as a substrate for which both $[\text{VO}(\text{3,5-DTBC})(\text{3,5-DBSQ})]_2$ and $\text{V}(\text{3,6-DTBC})_2(\text{3,6-DBSQ})$ function as effective precatalysts en route to intradiol and extradiol dioxygenase products. The use of the $\text{H}_2(\text{3,6-DTBC})$ substrate gives much less (1–2% vs. >9%) of the benzoquinone autoxidation product in comparison to $\text{H}_2(\text{3,5-DTBC})$, suggesting that the autoxidation pathway is significantly slowed relative to the dioxygenase pathway by using this sterically more hindered substrate.
- The choice of $\text{H}_2(\text{3,5-DTBC})$ vs. $\text{H}_2(\text{3,6-DTBC})$ substrate dictates whether the major observed dioxygenase product is a result of intradiol or extradiol cleavage: the $\text{H}_2(\text{3,5-DTBC})$ substrate gives >40% of an intradiol dioxygenase product while the $\text{H}_2(\text{3,6-DTBC})$ substrate results in >69% of an extradiol dioxygenase product with either $[\text{VO}(\text{3,5-DTBC})(\text{3,5-DBSQ})]_2$ or $\text{V}(\text{3,6-DTBC})_2(\text{3,6-DBSQ})$. In addition, no spiro product is observed with the $\text{H}_2(\text{3,6-DTBC})$ substrate presumably due to steric hindrance of the para-oriented (vs. meta-oriented with the $\text{H}_2(\text{3,5-DTBC})$ substrate) *tert*-butyl groups.
- EPR studies of $\text{H}_2(\text{3,6-DTBC})$ plus $[\text{VO}(\text{3,5-DTBC})(\text{3,5-DBSQ})]_2$ or $\text{V}(\text{3,6-DTBC})_2(\text{3,6-DBSQ})$ show that the same EPR spectra are observed throughout the reaction, but they occur at different reaction times depending on which precatalyst is used. The six-line hyperfine spectrum observed with both $[\text{VO}(\text{3,5-DTBC})(\text{3,5-DBSQ})]_2$ and $\text{V}(\text{3,6-DTBC})_2(\text{3,6-DBSQ})$ is hypothesized to result from the formation of free semiquinone radical. The different EPR spectra and different major products in comparison to those observed with the $\text{H}_2(\text{3,5-DTBC})$ substrate, suggests that $\text{H}_2(\text{3,6-DTBC})$ is oxygenated by a different mechanism than seen for $\text{H}_2(\text{3,5-DTBC})$.
- The ca. one to two orders of magnitude slower dioxygenase activity of $[\text{MoO}(\text{3,5-DTBC})]_2$, and much lower yields of the

desired dioxygenase products plus high yields of undesired benzoquinone autooxidation product, reveal that a d^0 vanadium complex containing a SQ ligand is important for the best dioxygenase catalysis that at least we have observed from the precatalysts tested.

4. Experimental

4.1. Reagents

$H_2(3,5\text{-DTBC})$ (Aldrich, 99%) was recrystallized three times from n-pentane under argon and stored in a Vacuum Atmosphere drybox ($O_2 \leq 5$ ppm). $H_2(3,6\text{-DTBC})$ was synthesized and recrystallized according to the modified literature procedure [11] and stored in the drybox. The solvent 1,2-dichloroethane (Aldrich, HPLC grade) was dried over preactivated 4 Å molecular sieves and stored in the drybox. $VO(acac)_2$ (Aldrich, 95%) and $Mo(CO)_6$ (Aldrich, 99.9+%) were used as received and stored in the drybox. The following were purchased where indicated and used as received: catechol (Aldrich, $\geq 99\%$), chloroform (Fisher, ACS grade), hexanes (Fisher, ACS grade), methanol (Fisher, HPLC grade), and n-pentane (Fisher, pesticide grade). Argon (99.985%) and oxygen (99.5%) gases were purchased from General Air and used as received.

4.2. Instrumentation

1H NMR were recorded in 5-mm o.d. tubes on a Varian Inova (J5-300) NMR spectrometer and referenced to the residual proton impurity in the deuterated solvent. EPR spectra were recorded on a Bruker EMX 200U EPR spectrometer using quartz 4-mm o.d. tubes and are referenced to 2,2-diphenyl-1-picrylhydrazyl (DPPH, $g = 2.0037$ g). GC analyses were performed on a Hewlett-Packard (HP) 5890 Series II gas chromatograph equipped with an FID detector and an SPB-1 capillary column (30 m, 0.25 mm i.d.) with the following temperature program: initial temperature, 200 °C (initial time, 2 min); heating rate, 2 °C/min; final temperature, 240 °C (final time, 3 min); FID detector temperature, 250 °C; injector temperature, 250 °C. An injection volume of 1 μ L was used. Electrospray ionization mass spectrometry analyses were performed on either a Thermo Finnigan LCQ Advantage Duo mass spectrometer or an Agilent model 6220 TOF mass spectrometer. Elemental analyses were performed by Galbraith Laboratories, Inc. (Knoxville, TN).

4.3. Preparation of $[VO(3,5\text{-DTBC})(3,5\text{-DBSQ})_2]$

The precatalyst $[VO(DTBC)(DBSQ)_2]$ was synthesized according to the published method [5,18] and characterized by EPR and UV/Vis. The synthesized product gave the characteristic 9-line EPR spectrum with a g -value of 2.006 in accord with the literature [18]. The UV/Vis under an inert atmosphere in toluene shows two absorbances at 298 and 660 nm in comparison to 294 and 668 nm reported in the literature [5]. Elemental analysis: calculated for $[VO(DTBC)(DBSQ)_2] \cdot CH_3OH$ [found]: C, 65.38 [65.26]; H, 8.09 [7.83]; V 9.73 [9.92].

4.4. Preparation of $V(3,6\text{-DTBC})_2(3,6\text{-DBSQ})$

$V(3,6\text{-DTBC})_2(3,6\text{-DBSQ})$ was synthesized according to a recently published method [11] and characterized by UV/Vis, EPR, single crystal X-ray diffraction, and elemental analysis. UV/Vis under an inert atmosphere in toluene shows an intense signal at 670 nm ($\epsilon = 33,000\text{--}38,000 M^{-1} cm^{-1}$). An EPR spectrum also in toluene and under an inert atmosphere shows a 9-line spectrum with $g = 2.0058$ and $A(^{51}V) = 3.47$ G and $A(^1H) = 4.53$ G. Elemental

analysis yields: calculated for $V(3,6\text{-DTBC})_2(3,6\text{-DBSQ}) \cdot CH_3OH$ [found]: C, 69.43 [69.91]; H, 8.67 [8.90]; V, 6.85 [6.58].

4.5. Preparation of $[MoO(3,5\text{-DTBC})_2]$

This precatalyst was synthesized according to the literature procedure [13]. In addition, the crude product was purified by recrystallization from hot n-pentane (recrystallization yield 40%) to yield a >95% pure product (by 1H NMR). Melting point: 301–302 °C. 1H NMR ($CDCl_3$) observed: 0.95, 1.30, 1.32, 1.55, 6.40, 6.77, 7.04, and 7.20 ppm; previously reported [13]: 0.95, 1.27, 1.28, 1.57, 6.81, 6.83, 7.08, and 7.11 ppm. Elemental analysis calculated for $[MoO(3,5\text{-DTBC})_2] \cdot 1.5(C_6H_5CH_3)$ [found]: C, 64.24 [64.03]; H, 7.46 [7.84]; Mo 15.4 [15.3].

4.6. Standard conditions O_2 -uptake experiments

These experiments were carried out as detailed elsewhere on a volume-calibrated oxygen-uptake line [4]. In a Vacuum Atmosphere drybox, ca. 1.8 mmol of $H_2(3,5\text{-DTBC})$ or $H_2(3,6\text{-DTBC})$ substrate was added to a 50 mL side-arm, round-bottomed, schlenk flask equipped with a septum and an egg-shaped 3/8-in. \times 3/16-in. Teflon-coated magnetic stir bar. Using a 10 mL gas-tight syringe, 8 mL of predried 1,2-dichloroethane was added to the flask. A vacuum adapter was attached and sealed with a Teflon stopcock, and the flask was brought out of the drybox. The flask was then connected to the oxygen uptake line via an O-ring joint, and the reaction solution was frozen in a dry-ice/ethanol bath (-76 °C) for 15 min. Two freeze-pump-thaw-fill cycles were performed using O_2 as the filling gas. The dry-ice/ethanol bath was then replaced with a temperature-controlled oil bath. The flask was then brought up to 40.0 ± 0.7 °C and allowed to equilibrate under stirring for 30 min. (Note: The catechol substrates, while initially kinetically insoluble, dissolve upon heating and stirring.) In the drybox, ca. 1–2 μ mol of the selected precatalyst was weighed into a 5 mL glass vial and dissolved in 0.2 mL of 1,2-dichloroethane. The catalyst solution was then mixed by repeatedly pulling the solution into and expelling from a 1 mL gas-tight syringe and then drawn into the syringe. The syringe was then inserted into a septum-capped 5 mL glass vial to protect the solution from air and brought out of the drybox. The catalyst solution was then injected into reaction flask through the sidearm and $t = 0$ was set. Pressure readings from the manometer were used to follow the reactions. Reactions were stopped when no further pressure loss was observed for ≥ 1 h.

4.7. Scaled-up O_2 -uptake experiments

The same procedure as detailed in Section 4.6 was employed except that ca. 1 g (4.5 mmol) of substrate and 5–6 μ mol of precatalyst is used in order to scale-up the amount of oxygenated product obtained.

4.8. $H_2(3,5\text{-DTBC})$ product identification

Product identification using GC was determined by co-injection of authentic materials [4]. In addition, mass spectrometry (MS) was employed to verify the formation of the products shown in Scheme 3.

4.9. $H_2(3,6\text{-DTBC})$ product separation and identification

Following the “Scale-Up O_2 -Uptake Experiments”, the main three $H_2(3,6\text{-DTBC})$ oxygenated products were separated in an analogous manner to the previously detailed separation of $H_2(3,5\text{-DTBC})$ products [4]. For details of this separation see Supporting Information. The $H_2(3,6\text{-DTBC})$ oxygenated products were then

characterized by ^1H and ^{13}C NMR, MS, and in the case of 3,6-di-*tert*-butyl-1-oxacyclohepta-3,5-diene-2,7-dione by single crystal X-ray diffraction (results are given in [Supporting Information](#)). The three main products making up ~90% of the mass balance are presented below along with their characterization.

4.9.1. 3,6-Di-*tert*-butyl-1-oxacyclohepta-3,5-diene-2,7-dione

GC–MS found for $\text{C}_{14}\text{H}_{20}\text{O}_3$, m/z 236 (M^+); ^1H NMR (CDCl_3): δ 1.25 (s, 18H, *t*-butyl), 6.40 (s, 2H, ring); ^{13}C NMR (CDCl_3): δ 29.4 (s, primary *t*-butyl), 36.3 (s, quaternary *t*-butyl) 126.0 (s, C4 and C5), 146.7 (s, C3 and C6), 161.6 (s, C2 and C7). Single crystals suitable for X-ray diffraction were obtained from hot pentane. The crystallographic data can be found in [Supporting Information](#).

4.9.2. 3,6-Di-*tert*-butyl-2H-pyran-2-one

GC–MS found for $\text{C}_{13}\text{H}_{20}\text{O}_2$, m/z 208 (M^+); ^1H NMR (CDCl_3): δ 1.25 (d, 18H, *t*-butyl), 5.94 (d, 1H, hydroxyl), 7.11 (d, 1H, ring); ^{13}C NMR (CDCl_3): δ 28.4 (s, primary *t*-butyl), 28.6 (s, primary *t*-butyl), 34.5 (s, quaternary *t*-butyl), 35.8 (s, quaternary *t*-butyl), 99.3 (s, C5), 133.5 (s, C4) 137.2 (s, C3), 161.0 (s, C2), 170.8 (s, C6).

4.9.3. 3,6-Di-*tert*-butyl-1,2-benzoquinone

GC–MS found for $\text{C}_{14}\text{H}_{20}\text{O}_2$, m/z 221 ($\text{M}+\text{H}^+$); ^1H NMR (CDCl_3): δ 1.25 (s, 18H, *t*-butyl), 6.78 (s, 2H, ring); ^{13}C NMR (CDCl_3): δ 29.4 (s, primary *t*-butyl), 32.5 (s, quaternary *t*-butyl), 134.2 (s, C4 and C5), 149.8 (s, C3 and C6), 181.4 (s, C1 and C2).

4.10. EPR during and following O_2 -uptake experiments

The same procedure as detailed in Section 4.6 was employed, except that: (i) ca. 5–8 μmol of the $\text{V}(\text{3,6-DTBC})_2(\text{3,6-DBSQ})$ or $[\text{VO}(\text{3,5-DTBC})(\text{3,5-DBSQ})]_2$ precatalyst was used, (ii) toluene was used as the solvent instead of 1,2-dichloroethane, with the toluene being frozen with liquid nitrogen, and (iii) the precatalyst was added to the $\text{H}_2(\text{DTBC})$ solution inside the drybox instead of by injection to the pre-stirred solution. The O_2 pressure loss was monitored by a mercury manometer [4]. Aliquots of reaction solution (0.3 mL) were drawn through the septum covered side-arm of the reaction flask at ca. 0.5 h after the pressure began to decrease and then ca. at every 10 Torr of pressure loss. The solution was also sampled again while still under the O_2 atmosphere through the reaction flask side-arm after no pressure loss was observed for >2 h.

Acknowledgement

These studies were supported by NSF grant CHE 9531110 to R.G.F.

Appendix A. Supplementary data

Supplementary data associated with this article can be found, in the online version, at doi:10.1016/j.molcata.2009.05.008.

References

- [1] C.L. Hill, I.A. Weinstock, *Nature* 388 (1997) 332–333.
- [2] (a) L. Que Jr., R.Y.N. Ho, *Chem. Rev.* 96 (1996) 2607–2624; (b) T. Funabiki, in: T. Funabiki (Ed.), *Catalysis by Metal Complexes*, vol. 19, Kluwer Academic Publishers, Dordrecht, The Netherlands, 1997, pp. 105–155; (c) H.-J. Krüger, in: B. Meunier (Ed.), *Biomimetic Oxidations Catalyzed by Transition Metal Complexes*, Imperial College Press, London, 2000, pp. 363–413; (d) R. Yamahara, S. Ogo, H. Masuda, Y. Watanabe, *J. Inorg. Biochem.* 88 (2002) 284–294; (e) M. Costas, M.P. Mehn, M.P. Jensen, L. Que Jr., *Chem. Rev.* 104 (2004) 939–986; (f) H.G. Jang, D.D. Cox, L. Que Jr., *J. Am. Chem. Soc.* 113 (1991) 9200–9204; (g) A. Dei, D. Gatteschi, L. Pardi, *Inorg. Chem.* 32 (1993) 1389–1395; (h) M. Ito, L. Que Jr., *Angew. Chem. Int. Ed.* 36 (1997) 1342–1344; (i) D.-H. Jo, L. Que Jr., *Angew. Chem. Int. Ed.* 39 (2000) 4284–4287; (j) M. Pascaly, M. Duda, F. Scheweppe, K. Zurlinden, F.K. Müller, B. Krebs, *J. Chem. Soc. Dalton Trans.* (2001) 828–837; (k) C.-H. Wang, J.-W. Lun, H.-H. Wei, M. Takeda, *Inorg. Chim. Acta* 360 (2007) 2944–2952; (l) R. Mayilmurugan, H. Stoeckli-Evans, M. Palaniandacar, *Inorg. Chem.* 47 (2008) 6645–6658.
- [3] (a) Y. Tatsuno, M. Tatsuda, S. Otsuka, *J. Chem. Soc. Chem. Commun.* (1982) 1100–1101; (b) Y. Tatsuno, C. Nakamura, T. Saito, *J. Mol. Catal.* 42 (1987) 57–66; (c) Y. Tatsuno, M. Tatsuda, S. Otsuka, K. Tani, *Chem. Lett.* (1984) 1209–1212; (d) U. Casellato, S. Tamburini, P.A. Vigato, M. Vidali, D.E. Fenton, *Inorg. Chim. Acta* 84 (1984) 101–104; (e) E. Roman, F. Tapia, M. Barrera, M.T. Garland, J.Y. Le Marouille, C. Giannotti, *J. Organomet. Chem.* 297 (1985) C8–C12; (f) B. Galeffi, M. Postel, A. Grand, P. Rey, *Inorg. Chim. Acta* 129 (1987) 1–5; (g) B. Galeffi, M. Postel, A. Grand, P. Rey, *Inorg. Chim. Acta* 160 (1989) 87–91; (h) Y. Nishida, H.Z. Kikuchi, *Naturforsch. B: Chem. Sci.* 44 (1989) 245–247; (i) U. Russo, B. Zarli, P. Zanonato, M. Vidali, *Polyhedron* 10 (1991) 1353–1361; (j) B.Y. Zhang, Y. Zhang, B.W. Chen, K. Wang, *Chin. Chem. Lett.* 8 (1997) 547–550.
- [4] H. Weiner, R.G. Finke, *J. Am. Chem. Soc.* 121 (1999) 9831–9842.
- [5] C.-X. Yin, R.G. Finke, *J. Am. Chem. Soc.* 127 (2005) 9003–9013.
- [6] C.-X. Yin, R.G. Finke, *J. Am. Chem. Soc.* 127 (2005) 13988–13996.
- [7] C.-X. Yin, Y. Sasaki, R.G. Finke, *Inorg. Chem.* 44 (2005) 8521–8530.
- [8] M. Matsumoto, K. Kuroda, *J. Am. Chem. Soc.* 104 (1982) 1433–1434.
- [9] (a) C. Bianchini, P. Frediani, F. Laschi, A. Meli, F. Vizza, P. Zanello, *Inorg. Chem.* 29 (1990) 3402–3409; (b) A. Vlcek Jr., *Chemtracts: Inorg. Chem.* 3 (1991) 275–280.
- [10] A. Nishinaga, *Catalysis by Metal Complexes*, vol. 19, Kluwer Academic Publishers, Dordrecht, The Netherlands, 1997, pp. 157–194.
- [11] A.M. Morris, C.G. Pierpont, R.G. Finke, *Inorg. Chem.* 48 (2009) 3496–3498.
- [12] (a) C.W. Lange, B.J. Conklin, C.G. Pierpont, *Inorg. Chem.* 33 (1994) 1276–1283; (b) C.-M. Liu, P. Restorp, E. Nordlander, C.G. Pierpont, *Chem. Commun.* (2001) 2686–2687; (c) C.-M. Liu, E. Nordlander, D. Schmech, R. Shoemaker, C.G. Pierpont, *Inorg. Chem.* 43 (2004) 2114–2124.
- [13] R.M. Buchanan, C.G. Pierpont, *Inorg. Chem.* 18 (1979) 1616–1620.
- [14] C.G. Pierpont, C.W. Lange, *Prog. Inorg. Chem.* 41 (1994) 331–442.
- [15] R.M. Buchanan, C.G. Pierpont, *J. Am. Chem. Soc.* 102 (1980) 4951–4957.
- [16] Y. Hitomi, M. Yoshida, M. Higuchi, H. Minami, T. Tanaka, T. Funabiki, *J. Inorg. Biochem.* 99 (2005) 755–763.
- [17] V.B. Vol'eva, A.I. Prokof'ev, A.Y. Karmilov, N.L. Komissarova, I.S. Belostotskaya, T.I. Prokof'eva, V.V. Ershov, *Russ. Chem. Bull.* 47 (1998) 1920–1923.
- [18] M.E. Cass, D.L. Green, R.M. Buchanan, C.G. Pierpont, *J. Am. Chem. Soc.* 105 (1983) 2680–2686.
- [19] (a) C.J. Winfield, Z. Al-Mahrizy, M. Gravestock, T.D.H. Bugg, *Perkin 1* (2000) 3277–3289; (b) T.D.H. Bugg, G. Lin, *Chem. Commun.* (2001) 941–952.
- [20] P. Barbaro, C. Bianchini, K. Linn, C. Mealli, A. Meli, F. Vizza, *Inorg. Chim. Acta* 198–200 (1992) 31–56.